



Phylogenetics and enzymology of plant quiescin sulfhydryl oxidase

Keren Limor-Waisberg^a, Assaf Alon^a, Tevie Mehlman^b, Deborah Fass^{a,*}

^a Department of Structural Biology, Weizmann Institute of Science, Rehovot 76100, Israel

^b Department of Biological Research Support, Weizmann Institute of Science, Rehovot 76100, Israel

ARTICLE INFO

Article history:

Received 30 August 2012

Revised 30 September 2012

Accepted 3 October 2012

Available online 12 October 2012

Edited by Takashi Gojobori

Keywords:

Disulfide bond formation

Thioredoxin

Flavin adenine dinucleotide

Multi-domain

Protein evolution

ABSTRACT

Quiescin Sulfhydryl Oxidase (QSOX), a catalyst of disulfide bond formation, is found in both plants and animals. Mammalian, avian, and trypanosomal QSOX enzymes have been studied in detail, but plant QSOX has yet to be characterized. Differences between plant and animal QSOXs in domain composition and active-site sequences raise the question of whether these QSOXs function by the same mechanism. We demonstrate that *Arabidopsis thaliana* QSOX produced in bacteria is folded and functional as a sulfhydryl oxidase but does not exhibit the interdomain electron transfer observed for its animal counterpart. Based on this finding, further exploration into the respective roles of the redox-active sites in plant QSOX and the reason for their concatenation is warranted. © 2012 Federation of European Biochemical Societies. Published by Elsevier B.V. All rights reserved.

1. Introduction

Disulfide bond formation in oxidative protein folding pathways is often catalyzed by two enzyme types, i.e., oxidoreductases and sulfhydryl oxidases, acting sequentially to transfer electrons from substrate thiols to terminal electron acceptors. Dithiol/disulfide oxidoreductases are often [1–3], but not always [4], members of the thioredoxin (Trx) fold superfamily. Sulfhydryl oxidases, together with functionally comparable enzymes that catalyze *de novo* disulfide bond formation but transfer electrons to substrates other than oxygen, belong to a number of different fold families [5–7]. One sulfhydryl oxidase family, found in the mitochondria [8] and endoplasmic reticulum [9], is known as Erv (Essential for respiration and viability) after the mitochondrial member. Erv domains comprise five helices and bind the cofactor flavin adenine dinucleotide (FAD) [10].

Although oxidoreductases and sulfhydryl oxidases are typically separate enzymes, a multi-domain protein family carrying out both these functions has also emerged. Quiescin sulfhydryl oxidase (QSOX) catalyzes both substrate oxidation and transfer of electrons to oxygen, via two redox-active CXXC motifs, one within a Trx domain and the second in an Erv domain [11]. Although missing in fungi, QSOX orthologs are found in metazoans, plants, and many protists [12] (Fig. 1). QSOX enzymes were first studied in mammalian systems [13–15], and metazoan and parasite QSOXs have since

been investigated in molecular mechanistic detail [16–21]. However, only a single report on a plant QSOX has appeared [22], and low turnover numbers were reported without further investigation.

Substantial dissimilarities in domain architecture and active-site motif sequences exist between plant and metazoan QSOXs. Plant QSOXs have a single Trx domain, whereas metazoan QSOXs have two adjacent Trx domains, the second being non-catalytic. Furthermore, the two intervening residues in both the Trx and Erv CXXC motifs differ between metazoans and plants, as previously reported [23]. Recently, the interdomain electron transfer mechanism of mammalian and trypanosomal QSOXs was demonstrated structurally and biochemically [20,21,24]. This research suggests that regions outside the two catalytic domains are important for the structure and dynamics of animal and parasite QSOXs. Whether plant QSOX, exhibiting different domain architecture and active-site motifs, has a similar catalytic mechanism and domain dynamics to those found in other QSOX enzymes should thus be evaluated. Here we report on the primary structure and biochemical activity of AtQSOX, from the model plant organism *Arabidopsis thaliana*.

2. Materials and methods

2.1. Phylogenetics

QSOX RefSeq entries were retrieved from the NCBI protein database, and duplicate entries and isoforms were removed. Alignments and neighbor-joining (NJ) trees were performed using

* Corresponding author. Fax: +972 8 934 4136.

E-mail address: deborah.fass@weizmann.ac.il (D. Fass).



Fig. 1. QSOX phylogenetic tree indicates uneven distribution of QSOX enzymes studied biochemically. Consensus maximum likelihood tree is based on concatenated Trx and Erv domains from QSOX enzymes. Metazoan QSOXs are highlighted in peach color, Trypanosomatidae in blue, Viridiplantae in green. Red dots indicate QSOX enzymes previously characterized biochemically (*R. norvegicus* QSOX [14], *G. gallus* [16,17], *B. taurus* [19], *H. sapiens* [23,24], and *T. brucei* [21]) or described herein (*A. thaliana*).

ClustalX [25] with default parameters (seed set to 111 and number of bootstrap to 1000). QSOX Erv domains were retrieved using the domain profile PS51324 (<http://www.expasy.org>). A QSOX-Trx specific user pattern: [LVEQ]-x(5)-C-[GEP]-[HFNDYA]-C-x(2)-[FYS]-x(3)-[WYFVI]-x(2)-[LVIAMF]-[AS]-X(20,36)-C-X(8)-P was used to retrieve QSOX Trx domains. The resulting Trx and Erv domains were concatenated. Maximum likelihood (ML) trees were constructed using Phylip [26] with Jones-Taylor-Thornton (JTT) probability models, and 100 replicates (seed was set to 9 and jumble to 3). A consensus tree was established using 'Consense' in the Phylip package.

2.2. Protein production and purification

A synthetic gene encoding *A. thaliana* QSOX1 (NCBI Accession number: NP_172955.1, corresponding to gene At1g15020) residues 34–443 was purchased (GeneScript) with codons optimized for expression in *Escherichia coli*. The resulting sequence was amplified using the primers (restriction sites underlined):

AtQSOXf: 5'-GGTCAGTACATATGTCGAATGTGGCGACCAGAAA-GATAATGCG-3' and AtQSOXr: 5'-TAGTGGATCCTCATTATTCACCGTTTTTTTTGTAGACCGACACCAG-3'. The PCR product was cloned into the pET15b vector (Novagen), encoding an amino-terminal His₆-tag and thrombin cleavage site. The plasmid was transformed into *E. coli* Origami B (DE3) pLysS cells (Novagen). Cells were grown at 37 °C to OD₆₀₀ ~0.5 in LB with 100 µg/ml ampicillin and 30 µg/ml chloramphenicol, then induced with 0.5 mM isopropyl β-D-1 thiogalactopyranoside and further grown for 36 h at 15 °C. AtQSOX was purified essentially as for other QSOX enzymes [24], except that gel filtration was performed in 20 mM sodium phosphate buffer, pH 7.5, 200 mM NaCl. *Homo sapiens* QSOX (HsQSOX1) and *Trypanosoma brucei* QSOX (TbQSOX) were prepared as described [24].

Protein-bound FAD concentration was determined by absorbance at 456 nm using an extinction coefficient of 12 400 M⁻¹cm⁻¹. Protein concentration was also calculated at 280 nm using an extinction coefficient of 98 160 M⁻¹cm⁻¹, which includes the absorbance of the FAD at this wavelength (21 300 M⁻¹cm⁻¹).

2.3. Thiol titers

AtQSOX thiol titer was determined by adding 0.2 mM 5,5'-dithiobis(2-nitrobenzoate) (DTNB) to 4.5 µM enzyme in 4.4 M guanidine-HCl and 50 mM sodium phosphate buffer (pH 7.5). Absorbance at 412 nm was recorded relative to a blank prepared identically but lacking AtQSOX, and the concentration of the resulting 2-nitro-5-thiobenzoate (TNB⁻) was determined using an extinction coefficient of 14 150 M⁻¹cm⁻¹. The calculated absorbance of TNB⁻ derived from one thiol per protein molecule under these conditions would be 0.06 ODU.

2.4. Analytical gel filtration

Purified enzymes were applied to an analytical grade Superdex™ 75 10/300 GL size exclusion column equilibrated with 50 mM sodium phosphate buffer (pH 7.5), 65 mM NaCl, 1 mM EDTA, and absorption was monitored at 450 nm.

2.5. Mass spectrometry

AtQSOX, treated with 10 mM *N*-ethylmaleimide prior to the addition of gel loading buffer containing SDS, was run on a 10% SDS-PAGE gel. The AtQSOX band was excised and subjected to in-gel enzymatic digestion with trypsin or a combination of chymotrypsin and AspN protease, without reduction and alkylation.

Peptide mixtures were extracted with 80% CH₃CN, 1% CF₃COOH, and solvent was evaporated in a vacuum centrifuge. The resulting peptide mixtures were reconstituted in 80% formic acid and diluted 1:10 with Milli-Q water. Liquid chromatography tandem mass spectrometry (LC–MS/MS) was performed on an LTQ Orbitrap (Thermo Fisher Scientific). Raw data files were searched with the MassMatrix software [27] against the predicted AtQSOX amino acid sequence.

2.6. Enzyme assays

AtQSOX activity was measured at 25 °C by monitoring oxygen consumption in a Clarke-type oxygen electrode (Hansatech Instruments Ltd.). Dithiothreitol (DTT) was prepared in 50 mM sodium phosphate buffer (pH 7.5), 65 mM NaCl, 1 mM ethylenediaminetetraacetic acid (EDTA) at 20–100X the final concentration for each measurement. AtQSOX was diluted into buffer, and reactions were initiated by injection of DTT to yield 1 ml total volume. Background oxygen consumption in the absence of enzyme was minimal at all DTT concentrations.

Experiments with maleimide-functionalized polyethylene glycol (mal-PEG) were performed by incubating 50 µl of 1 µM enzyme with DTT for 10 s, then adding 15 µl trichloroacetic acid (TCA). After incubation at 4 °C for 1 h, samples were spun at 10,000xg for 10 min. Supernatant was removed, and the protein pellet washed three times with 500 µl ice-cold acetone and centrifuged for 5 min at 10,000xg after each wash. Acetone was removed and the pellet left to air-dry. The mal-PEG was prepared at a concentration of 10 mM in phosphate buffered saline, de-salted over a PD-10 column (GE Healthcare) to remove any unconjugated maleimide, and diluted 1:10 into gel loading buffer, which was then used to resuspend the TCA-precipitated pellets for application to a polyacrylamide gel.

3. Results

3.1. QSOX phylogenetics and redox-active motifs

The divergence of plant and metazoan QSOXs is most evident in their domain composition. Whereas metazoan QSOXs have two adjacent Trx domains, plants and protists have a single Trx. Phylogenetic trees emphasize this separation, with metazoan and plant QSOXs clearly clustered apart, as expected (Fig. 2). Metazoan QSOXs separate into three defined branches: arthropod QSOX, and QSOX1 and QSOX2 in non-arthropods. Most plants contain a single QSOX gene and follow a continuous branch starting from the unicellular Chlorophyta to multicellular Bryophyta, Lycopodiophyta, monocotyledons, and eudicotyledons. The two AtQSOX paralogs likely result from a recent duplication at the genus level. AtQSOX1 (hereafter AtQSOX) and AtQSOX2 share 78% amino acid identity.

AtQSOX used in this study has 16 cysteine residues. Six cysteines are present in three conserved CXXC motifs: one in the Trx domain, one in the Erv domain, and one just downstream of the Erv domain (Fig. 3A). Differences between plant and metazoan CXXC motifs were previously reported [23]. Whereas the metazoan Trx domain motif has the pattern CGXC (typically CGHC in chordates), most plants have a CPXC sequence (CPAC in higher plants). The Erv CXXC is somewhat more varied, with chordates exhibiting a C[RK][DE]C pattern and higher plants C[DE][DE]C, specifically CDDC in AtQSOX. QSOX alignments further reveal that plant QSOXs are richer in cysteines than metazoan QSOXs. This trend increases with plant complexity, with eudicotyledons richest in cysteines (Fig. 3B). The C₂₅₇/C₂₆₂ cysteine pair is seen only in *Arabidopsis* species. Interestingly, only one of these cysteines is present in QSOXs

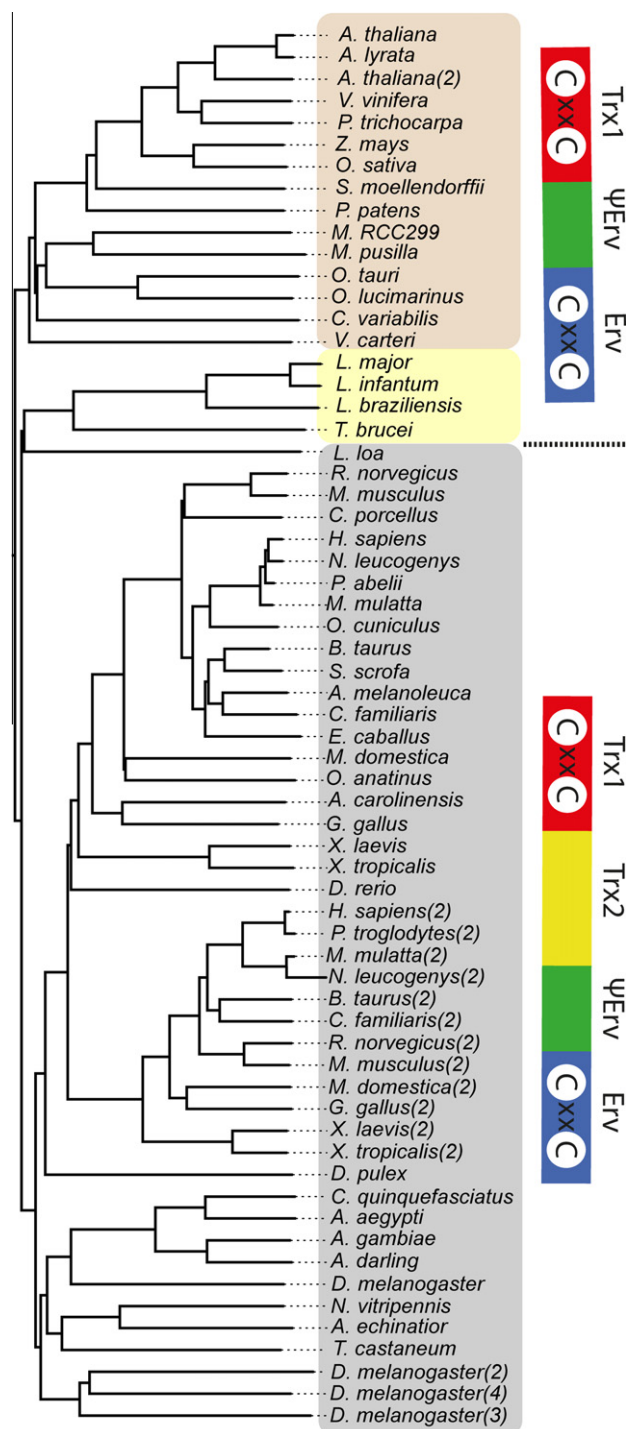


Fig. 2. QSOX neighbor-joining tree shows the major partitioning of QSOX enzymes into those containing and lacking a Trx2 domain. Metazoans are highlighted in gray. Trypanosomatidae in yellow, Viridiplantae in pink. Maps of QSOX domain composition are indicated to the right. Trx1 is a redox-active thioredoxin fold. Trx2 is a thioredoxin fold lacking redox-active cysteines. The ψ Erv region has helix topology similar to that of the Erv domain but lacks redox-active cysteines and FAD-binding capability [29]. Erv refers to the Erv family sulphhydryl oxidase fold with redox-active cysteines and an FAD cofactor.

of other eudicotyledons, such as *Vitis vinifera* and *Populus trichocarpa*, which consequently have an odd number of cysteines in their ψ Erv/Erv regions. No cysteine corresponding to either C₂₅₇ or C₂₆₂ is present in QSOXs from lower plants. The C₃₃₀/C₃₅₀ cysteine pair appears in monocotyledons and eudicotyledons but

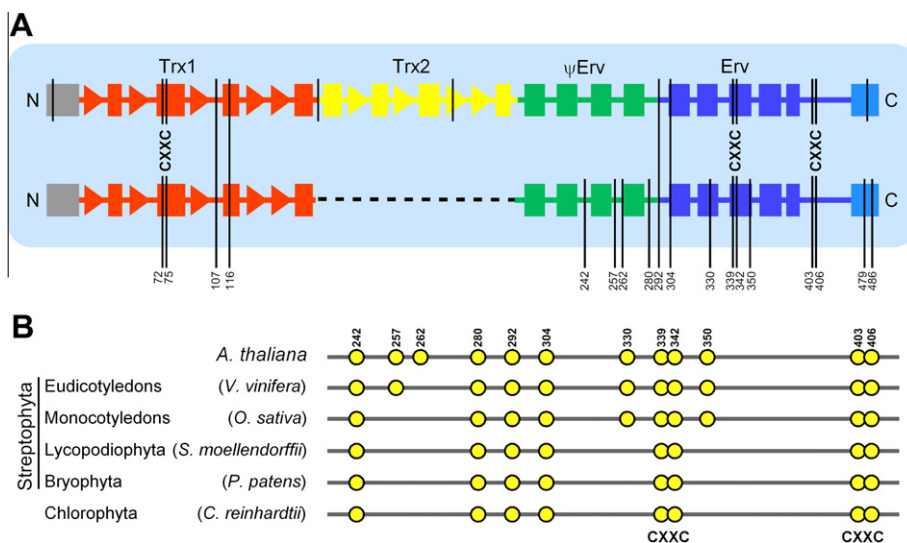


Fig. 3. QSOX domain organization and plant-specific cysteine residues. Domains are as described in Fig. 2. Cysteine numbering is according to AtQSOX. (A) Known or predicted secondary structural maps (rectangle = helix; triangle = strand) of mammalian QSOX (upper) and AtQSOX (lower) are juxtaposed. The positions of common cysteines are indicated by lines extending over both maps. Cysteines present in only plant or mammalian QSOXs are represented with shorter lines. (B) Cysteines, represented by yellow circles, are compared across various plant species for the ψ Erv/Erv segment.

is absent from lower plants, and the tight correlation suggests they form a disulfide bond.

3.2. Expression and purification of AtQSOX

The AtQSOX coding sequence lacking the signal peptide and transmembrane segment was optimized for expression in *E. coli*. The resulting recombinant protein, containing a cleavable amino-terminal His₆-tag, was expressed in soluble form in bacterial cytosol. Purified protein yields were low, typically less than 0.5 mg per liter of culture.

AtQSOX migration on SDS-PAGE corresponded to the predicted molecular weight of \sim 47 kDa (Fig. 4A). When studied by analytical equilibrium ultracentrifugation, AtQSOX showed a slight tendency toward self-association, which complicated data analysis (not shown). When assessed by analytical gel filtration, AtQSOX migrated at a position roughly consistent with a monomer but shifted slightly toward higher solution molecular weight, or a greater aspect ratio, relative to other QSOX enzymes. Furthermore, AtQSOX exhibited an asymmetrical peak in the chromatogram, whereas other QSOXs showed symmetrical peaks (Fig. 4B).

3.3. UV/Vis spectroscopy, thiol titers, and disulfide connectivity

Purified AtQSOX showed a typical flavin absorbance spectrum (Fig. 4C), with a maximum at 456 nm similar to HsQSOX1 [20]. The ratio of protein concentration calculated from absorbance at 456 nm, using the extinction coefficient of the FAD, vs. 280 nm, using the extinction coefficients of protein aromatic residues and the contribution of the FAD at this wavelength, was 1.0, consistent with a protein population fully loaded with co-factor. The absorbance measured upon reaction of AtQSOX with DTNB in either the native or denatured states ($Abs_{412\text{ nm}}$ 0.013 and 0.018, respectively) indicated less than one free thiol per protein molecule (calculated to give $Abs_{412\text{ nm}}$ 0.06), demonstrating that all cysteines were oxidized in the recombinant AtQSOX preparation. Tandem mass spectrometry (LC-MS/MS) was used to confirm protein identity and determine cysteine pairing (Supplementary Table). The output data, showing 96% coverage of the recombinant AtQSOX amino acid sequence, indicated unambiguously the following crosslinks: C₇₂-C₇₅, C₁₀₇-C₁₁₆, C₂₅₇-C₂₆₂, C₂₉₂-C₃₀₄, C₃₃₀-C₃₅₀, C₃₃₉-C₃₄₂, and C₄₀₃-C₄₀₆ (Fig. 5). In addition, the data strongly supported the presence of a crosslink between C₂₄₂ and C₂₈₀, but C₂₈₀

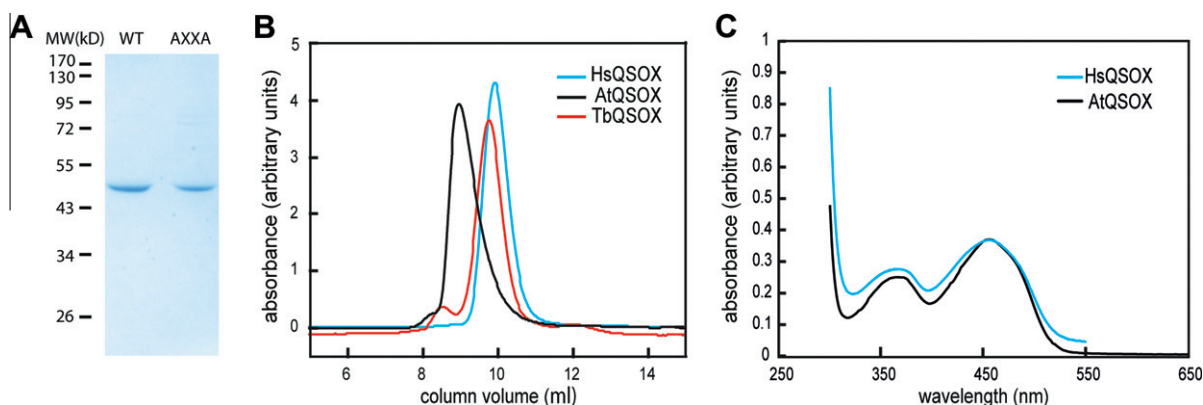


Fig. 4. Purification and characterization of recombinant AtQSOX. (A) Purified AtQSOX (WT) and AtQSOX C72A/C75A (AXXA) were analyzed under non-reducing conditions by SDS-PAGE stained with Coomassie. (B) Analytical gel filtration profile of AtQSOX vs. other QSOX enzymes. (C) Absorbance spectrum of AtQSOX vs. HsQSOX1 (HsQSOX).

was also detected in a conflicting crosslink with C₁₀₇. Inspection of the fragment ions for the competing crosslink showed poor y ion series, despite the excellent quality of the data for all other crosslinks, including C₂₄₂–C₂₈₀. It should be noted that the plethora of trypsin recognition sites to either side of C₂₄₂ (sequence RRC₂₄₂R) may limit the options for detecting a crosslink between C₂₄₂ and C₂₈₀ after trypsin digestion. No peptides containing C₂₄₂ or C₂₈₀ were observed following digestion with chymotrypsin and Asp-N.

3.4. Catalytic activity of AtQSOX

In contrast to other QSOXs tested in parallel, AtQSOX showed negligible oxidation of the model protein substrate reduced, unfolded RNase A (not shown). Sulfhydryl oxidase activity was observed, however, on the small-molecule substrate DTT. Turnover numbers, monitored by oxygen consumption, were on the same order of magnitude as other QSOXs [20,21]. However, other QSOXs have K_M values for DTT in the ~100 μ M range, whereas the activity of AtQSOX on DTT did not fully saturate up to a substrate concentration of 100 mM (Fig. 6A). High K_M values for DTT were seen previously for QSOXs lacking Trx CXXC cysteines ([21] and unpublished data). Under these conditions, DTT directly reduces the FAD-proximal, Erv CXXC disulfide. Our observations suggest that recombinant AtQSOX, though possessing Trx CXXC cysteines, catalytically oxidizes DTT directly at the FAD-proximal cysteines and not via the shuttle mechanism seen in other QSOX orthologs. Indeed, the C72A/C75A AtQSOX double-mutant showed activity indistinguishable from wild type (Fig. 6A).

The apparent lack of participation of the AtQSOX Trx CXXC in catalysis could be due to either of two scenarios. One possibility is that DTT reduces the Trx CXXC, but that the electrons are not further shuttled to the Erv domain. Alternatively, the Trx CXXC is resistant to reduction by DTT and thus does not acquire electrons. To distinguish between these possibilities, AtQSOX and the C72A/C75A double-mutant were incubated for short periods with varying concentrations of DTT, and the presence of free cysteine thiols in each enzyme variant was probed. Specifically, solutions of DTT and enzyme were rapidly acidified by addition of TCA, which blocked further redox activity and precipitated the protein. Enzymes were resuspended in the presence of mal-PEG of molecular weight 5 kDa. In this manner, unpaired cysteines were modified, and modified protein migrated far above fully oxidized protein on a gel. A substantial fraction of wild-type AtQSOX reacted with mal-PEG after treatment with even low DTT concentrations, whereas AtQSOX C72A/C75A remained un-modified over a wide range of DTT concentrations (Fig. 6B). We conclude that the AtQSOX Trx CXXC is readily reduced by DTT, but that electrons are not efficiently transferred from the Trx to the Erv domain.

The apparently poor dithiol/disulfide exchange between the two AtQSOX redox-active domains, coupled with a slight tendency to self-associate, raises the possibility that, unlike other QSOX enzymes, AtQSOX relies on intermolecular electron transfer for activity. However, the *A. thaliana* enzyme showed no concentration-dependent changes in turnover number between 100 and 800 nM enzyme (Fig. 6C), suggesting that no functionally significant changes in self-association occur over this concentration range.

4. Discussion

Protein disulfide isomerase (PDI) family oxidoreductases, like QSOX enzymes, often contain tandem Trx domains [1]. Unlike QSOXs, however, PDIs have highly variable domain contents in different organisms. The PDI family also has widely different numbers of paralogs in different organisms, suggesting niche roles in oxidative folding of species-specific substrates. In contrast, QSOX domain composition is relatively well conserved. The tighter constraints on the QSOX family are likely due to the requirement, at least in metazoan and protist QSOXs, for interdomain electron transfer in the enzyme reaction cycle [18,20,21,24]. The amino-terminal, redox-active Trx domain of QSOX must be tethered to the remainder of the protein in a manner that allows its CXXC motif to undergo dithiol/disulfide exchange with the FAD-proximal CXXC of the Erv domain.

This relatively conserved domain composition lends itself to speculation regarding the route by which contemporary QSOXs appeared. In principle, plant and animal QSOXs could have arisen by independent fusion events between Trx and Erv domains. In this case, plant QSOX may have arisen directly as a single-Trx enzyme, and animal QSOX with tandem Trx domains. Another scenario is that both plant and animal QSOXs came from a single precursor, involving a tandem Trx fusion with an Erv segment, but that the plant lineage lost a Trx domain. Alternatively, the precursor contained only a single Trx domain, and the metazoan lineage subsequently gained a second Trx. It has been noted that particular composite domain architectures are most likely to have arisen from single fusion events [28]. However there are exceptions to this generalization, and the evolutionary relationship between plant and animal QSOXs remains an open question.

Some parasite QSOXs have single Trx domains like plant QSOXs, but these enzymes share low sequence identity with both plant and animal QSOXs. Interestingly, although TbQSOX is different in domain organization and active-site sequences from mammalian QSOX, it has similar catalytic properties. For example, the k_{cat} of TbQSOX [24] and HsQSOX1 [20] are 600 min^{-1} and 640 min^{-1} , respectively, and both enzymes show sub-millimolar K_M for DTT. These similarities between highly divergent QSOX enzymes suggested that all QSOXs may have similar catalytic properties, regardless of their phylogenetic assignment.

A previous study of AtQSOX produced in yeast [22] reported a turnover number of 14 min^{-1} on 250 μ M DTT, about 2% the activity typically observed for mammalian and parasite QSOXs. This discrepancy could have been due to lower absolute activity (i.e., k_{cat} value) of plant vs. animal QSOX, different substrate preference (i.e., higher K_M for DTT), or non-optimal preparation of the plant enzyme. To resolve this question, we produced recombinant plant QSOX and characterized thoroughly its folding, monodispersity, and enzymatic activity. We observed that AtQSOX is oxidized, fully loaded with cofactor, and displays a uniform and structurally justifiable disulfide connectivity. Purified AtQSOX is not cleanly monodisperse like other QSOXs, but rather has a slight tendency toward self-association, observed by analytical gel filtration and ultracentrifugation. However, we see no decrease in k_{cat} with increasing enzyme concentrations, as would be expected if aggregation were interfering with activity. Neither do we observe

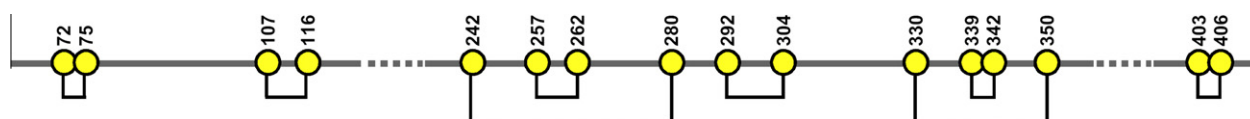


Fig. 5. Disulfide connectivity of AtQSOX best supported by mass spectrometry data (Supplementary Table). Numbering indicates the position of each AtQSOX cysteine residue, as in Fig. 3.

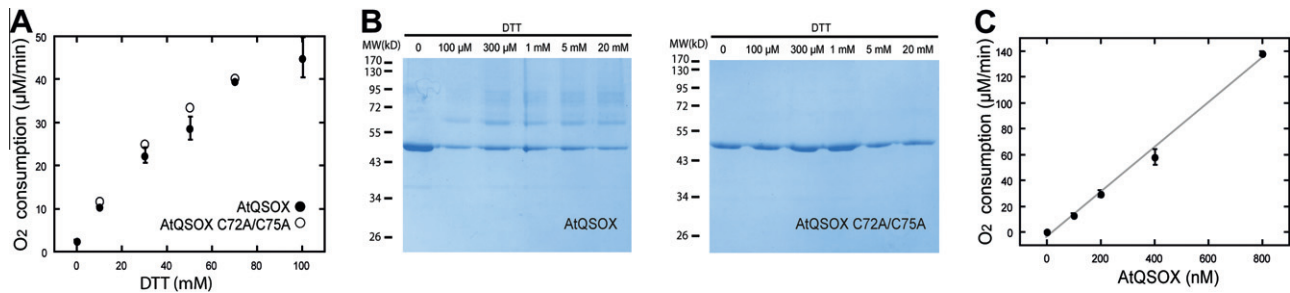


Fig. 6. Enzymatic activity of AtQSOX. (A) Activity of AtQSOX (●) or AtQSOX C72A/C75A (○) on various concentrations of DTT, measured by oxygen consumption. AtQSOX results are averages and standard deviations of three measurements. (B) Modification of AtQSOX and AtQSOX C72A/C75A with mal-PEG after incubation with the indicated concentrations of DTT. Each mal-PEG addition results in a shift on SDS-PAGE comparable to 15 kD of protein. (C) Activity as a function of AtQSOX concentration, measured on 20 mM DTT, is linear over the indicated enzyme concentration range.

an increase in activity with increasing enzyme concentrations, as would be expected if activity depended on multimerization. We therefore conclude that plant and animal QSOXs have significantly different properties. Based on the observation that, after incubation with DTT, AtQSOX shows reactivity with mal-PEG but AtQSOX C72A/C75A does not, we conclude that the AtQSOX Trx domain is readily reduced by DTT. However, turnover numbers quantified by reduction of molecular oxygen do not reflect reactivity of the Trx domain if there is no redox communication with the Erv domain. The previous study of AtQSOX [22] monitored activity at DTT concentrations far below the K_M . In this study we show that recombinant AtQSOX does not apparently transfer electrons from its Trx domain to its Erv domain to accomplish rapid oxidation of highly reducing model dithiol substrates, and the measured sulfhydryl oxidase activity reflects the activity of the Erv domain alone, limited by a high K_M for DTT and likely other thiol substrates.

A number of potential explanations exist for lack of apparent redox communication between the AtQSOX Trx and Erv domains. As described above, we established that the Trx domain can acquire electrons. While we cannot rule out partial mis-folding or lack of an essential post-translational modification as the barrier to electron relay, one possibility is that the Trx CPAC motif fails to transfer electrons to the Erv CDDC motif due to inherent lack of reactivity between these sites. Alternatively, these sites may be chemically capable of electron transfer, but sterically restricted from interacting in the AtQSOX structure. For example, the interdomain linker may be too short or positioned inappropriately for interdomain redox communication. One experiment to distinguish these possibilities requires the Trx and Erv fragments of AtQSOX to be produced separately, which we have not yet accomplished. It was previously observed that 250 μM of a HsQSOX1 Trx1/Trx2 fragment could be supplied to 100 nM HsQSOX1 ψErv/Erv fragment to achieve reaction rates comparable to 100 nM intact HsQSOX1 [24]. If similar concentrations of AtQSOX Trx domain supplied to AtQSOX ψErv/Erv would yield turnover numbers of ~500 in the presence of sub-millimolar DTT, one would conclude that the AtQSOX sites are sterically unable to interact in the intact monomeric enzyme but chemically competent for electron transfer. In this case, perhaps tethering to the membrane via the transmembrane segment, absent from this and the previous [22] study of recombinant AtQSOX, contributes to intermolecular redox communication from one Trx domain to the Erv domain of a neighboring molecule. Regardless of whether the AtQSOX Trx and Erv redox-active sites are chemically or sterically incompatible, it remains to be determined whether there is functional significance to their presence within the same protein.

5. Author contributions

K.L.W. and A.A. prepared and purified the protein. K.L.W. performed phylogenetic analyses and enzymatic assays. T.M. analyzed

mass spectrometry data. All authors planned experiments and discussed interpretation of the results. K.L.W. and D.F. wrote the manuscript.

Acknowledgments

We thank Iris Grossman for testing AtQSOX in RNase A oxidation assays and Dalit Merhav for preparation of samples for mass spectrometry.

This study was supported by the Israel Science Foundation and by the Kimmelman Center for Macromolecular Assemblies.

Appendix A. Supplementary data

Supplementary data associated with this article can be found, in the online version, at <http://dx.doi.org/10.1016/j.febslet.2012.10.003>.

References

- [1] Appenzeller-Herzog, C. and Ellgaard, L. (2008) The human PDI family: versatility packed into a single fold. *Biochim. Biophys. Acta* 1783, 535–548.
- [2] Berndt, C., Lillig, C.H. and Holmgren, A. (2008) Thioredoxins and glutaredoxins as facilitators of protein folding. *Biochim. Biophys. Acta* 1783, 641–650.
- [3] Inaba, K. (2009) Disulfide bond formation system in *Escherichia coli*. *J. Biochem.* 146, 591–597.
- [4] Mesecke, N., Terziyska, N., Kozany, C., Baumann, F., Neupert, W., Hell, K. and Herrmann, J.M. (2005) A disulfide relay system in the intermembrane space of mitochondria that mediates protein import. *Cell* 121, 1059–1069.
- [5] Gross, E., Kastner, D.B., Kaiser, C.A. and Fass, D. (2004) Structure of Ero1p, source of disulfide bonds for oxidative protein folding in the cell. *Cell* 117, 601–610.
- [6] Li, W., Schulman, S., Dutton, R.J., Boyd, D., Beckwith, J. and Rapoport, T.A. (2010) Structure of a bacterial homologue of vitamin K epoxide reductase. *Nature* 463, 507–512.
- [7] Gross, E., Sevier, C.S., Vala, A., Kaiser, C.A. and Fass, D. (2002) A new FAD-binding fold and intersubunit disulfide shuttle in the thiol oxidase Erv2p. *Nat. Struct. Biol.* 9, 61–67.
- [8] Lee, J., Hoffhaus, G. and Lisowsky, T. (2000) Erv1p from *Saccharomyces cerevisiae* is a FAD-linked sulfhydryl oxidase. *FEBS Lett.* 477, 62–66.
- [9] Sevier, C.S., Cuzzo, J.W., Vala, A., Aslund, F. and Kaiser, C.A. (2001) A flavoprotein oxidase defines a new endoplasmic reticulum pathway for biosynthetic disulfide bond formation. *Nat. Cell Biol.* 3, 874–882.
- [10] Fass, D. (2008) The Erv family of sulfhydryl oxidases. *Biochim. Biophys. Acta* 1783, 371–378.
- [11] Coppock, D.L., Cina-Poppe, D. and Gilleran, S. (1998) The quiescin Q6 gene (QSCN6) is a fusion of two ancient gene families: thioredoxin and ERV1. *Genomics* 54, 460–468.
- [12] Thorpe, C., Hooper, K.L., Raje, S., Glynn, N.M., Burnside, J., Turi, G.K. and Coppock, D.L. (2002) Sulfhydryl oxidases: emerging catalysts of protein disulfide bond formation in eukaryotes. *Arch. Biochem. Biophys.* 405, 1–12.
- [13] Janolino, V.G. and Swaisgood, H.E. (1975) Isolation and characterization of a sulfhydryl oxidase from bovine milk. *J. Biol. Chem.* 250, 2532–2538.
- [14] Ostrowski, M.C. and Kistler, W.S. (1980) Properties of a flavoprotein sulfhydryl oxidase from rat seminal vesicle secretion. *Biochem.* 19, 2639–2645.
- [15] Takamori, K., Thorpe, J.M. and Goldsmith, L.A. (1980) Skin sulfhydryl oxidase. Purification and some properties. *Biochim. Biophys. Acta* 615, 309–323.

- [16] Hooper, K.L. and Thorpe, C. (1999) Egg white sulfhydryl oxidase: kinetic mechanism of the catalysis of disulfide bond formation. *Biochem.* 38, 3211–3217.
- [17] Hooper, K.L., Sheasley, S.L., Gilbert, H.F. and Thorpe, C. (1999) Sulfhydryl oxidase from egg white. A facile catalyst for disulfide bond formation in proteins and peptides. *J. Biol. Chem.* 274, 22147–22150.
- [18] Raje, S. and Thorpe, C. (2003) Inter-domain redox communication in flavoenzymes of the quiescin/sulfhydryl oxidase family: role of a thioredoxin domain in disulfide bond formation. *Biochem.* 42, 4560–4568.
- [19] Jaje, J., Wolcott, H.N., Faduqba, O., Cripps, D., Yang, A.J., Mather, I.H. and Thorpe, C. (2007) A flavin-dependent sulfhydryl oxidase in bovine milk. *Biochem.* 46, 13031–13040.
- [20] Heckler, E.J., Alon, A., Fass, D. and Thorpe, C. (2008) Human quiescin-sulfhydryl oxidase, QSOX1: probing internal redox steps by mutagenesis. *Biochem.* 47, 4955–4963.
- [21] Kodali, V.K. and Thorpe, C. (2010) Quiescin sulfhydryl oxidase from *Trypanosoma brucei*: catalytic activity and mechanism of a QSOX family member with a single thioredoxin domain. *Biochem.* 49, 2075–2085.
- [22] Alejandro, S., Rodríguez, P.L., Bellés, J.M., Yenush, L., García-Sánchez, M.J., Fernández, J.A. and Serrano, R. (2007) An Arabidopsis quiescin-sulfhydryl oxidase regulates cation homeostasis at the root symplast-xylem interface. *EMBO J.* 26, 3203–3215.
- [23] Heckler, E.J., Rancy, P.C., Kodali, V. and Thorpe, C. (2008) Generating disulfides with the Quiescin-sulfhydryl oxidases. *Biochim. Biophys. Acta* 1783, 567–577.
- [24] Alon, A., Grossman, I., Gat, Y., Kodali, V.K., DiMaio, F., Mehlman, T., Haran, G., Baker, D., Thorpe, C. and Fass, D. (2012) The dynamic disulphide relay of quiescin sulfhydryl oxidase. *Nature* 488, 414–418.
- [25] Larkin, M.A., Blackshields, G., Brown, N.P., Chenna, R., McGettigan, P.A., McWilliam, H., Valentin, F., Wallace, I.M., Wilm, A., Lopez, R., Thompson, J.D., Gibson, T.J. and Higgins, D.G. (2007) Clustal W and Clustal X version 2.0. *Bioinformatics* 23, 2848–2947.
- [26] Felsenstein, J. (2005) PHYLIP (Phylogeny Inference Package) version 3.6. *Distributed by the author. Department of Genome Sciences, University of Washington, Seattle.*
- [27] Xu, H., Zhang, L. and Freitas, M.A. (2008) Identification and characterization of disulfide bonds in proteins and peptides from tandem MS data by use of the MassMatrix MS/MS search engine. *J. Proteome Res.* 7, 138–144.
- [28] Kummerfeld, S.K. and Teichmann, S.A. (2005) Relative rates of gene fusion and fission in multi-domain proteins. *Trends Genet.* 21, 25–30.
- [29] Alon, A., Heckler, E.J., Thorpe, C. and Fass, D. (2010) QSOX contains a pseudodimer of functional and degenerate sulfhydryl oxidase domains. *FEBS Lett.* 584, 1521–1525.